RARE METALS
Vol. 29, No. 2, Apr 2010, p. 154
DOI: 10.1007/s12598-010-0027-1

Effects of $Ti_{0.5}Al_{0.5}N$ coatings on the protecting against oxidation for titanium alloys

RU Qiang[a] and HU Shejun[b]

[a] *Laboratory of Quantum Information Technology, School of Physics and Telecommunication Engineering, South China Normal University, Guangzhou 510006, China*
[b] *Department of Mathematics and Physics, Wuyi University, Jiangmen 529020, China*

Received 24 March 2009; received in revised form 27 May 2009; accepted 29 May 2009

Abstract

$Ti_{0.5}Al_{0.5}N$ coatings were deposited on TC11 (Ti-6.5Al-3.5Mo-1.5Zr-0.3Si) and silicon substrates using a cathode arc ion-plating system. The microstructure, composition, phase structure, and oxidation-resistance of the alloys and nitride coatings were investigated by scanning electron microscopy, X-ray diffraction, transmission electron microscopy, Auger electron spectroscopy, and thermal analyzer. The results show that the oxidation resistance of the titanium alloy is relatively limited; the compound structures of Ti mixed with Al oxides are formed during the heating process. The phases of the $Ti_{0.5}Al_{0.5}N$ coatings are composed of a TiN solid solution phase. The oxidation kinetics obeys the parabolic law. During the oxidation process, the selective oxidation of Al occurs, thus protecting the underlying coating and substrate.

Keywords: titanium alloy; TiAlN; oxidation resistance; ion plating

1. Introduction

Titanium alloys with excellent mechanical properties and superior corrosion resistance have been widely used in many fields, such as in the aviation-aerospace industry, medicine-chemical engineering and bio-engineering. However, as the temperature in air increases, alloys are easily destroyed by oxygen reaction and the formation of the brittlement phase, which seriously weaken their anti-oxidation and mechanical properties [1]. Thus, relatively poor oxidation resistance in the evaluated temperature is the critical factor that always directly limits practical application. Current studies show that the protective coating technique is a simple and effective method to partly resolve these problems [2-3], but some disadvantages of the coating process are also revealed, for instance, hydrogen embrittlement produced by the wet method, micro-crack sensitivity generated by laser cladding, brittle phases and the Kirkendall effect caused by elements interdiffusion [4-5].

The vacuum arc ion plating technique has great advantages with respect to metal nitride hard coating, and various hard coating systems are also successfully developed and commercially employed with nitride systems [6]. Among these coatings, the Ti-Al-N system offers superior performance for metal machining and fabrication applications, exhibiting improved tribological properties and elevated oxidation [7]. Current studies mostly focus on the protection of high-speed steel, die steel, and hard carbide tools [8-9], while the protection of high temperature titanium alloys is not familiar to some researchers. The investigation in this paper aims to develop suitable protective coatings for the titanium alloy. The effect of aluminum added to the Ti-N matrix, the microstructure and the thermal stability characteristics of $Ti_{0.5}Al_{0.5}N$ coatings are discussed.

2. Experimental

Titanium aluminum nitride coatings were prepared on TC11 (Ti-6.5Al-3.5Mo-1.5Zr-0.3Si) sheets and silicon slices by cathodic vacuum arc ion plating. The treated TC11 alloys were cut into sheets with dimensions of 20 mm × 15 mm × 2.5 mm and polished to mirror [10]. The substrates were ultrasonically cleaned using a decontaminating agent, alcohol, and acetone sequentially. The pure Ti target and $Ti_{0.5}Al_{0.5}$ (atomic ratio) alloy target were used. The vacuum degree was 0.6 Pa, the bias voltage was −200 V, and the cathode target current was 70 A. The nominal component of the obtained nitride coating was $Ti_{0.5}Al_{0.5}N$. The oxidation resistance was evaluated by cyclic oxidation test in air; the heating conditions were 650°C / 100 h, 700°C / 100 h,

Corresponding author: RU Qiang **E-mail:** rq7702@yeah.net

800°C / 10 h, and 800°C / 30 h. The morphologies of the specimens were observed with an atomic force microscope (AFM, SPM-9500J3) and NoVaTM SEM 430 and a Philip XL30FEG field emission scanning electron microscope, while the phases' structures were analyzed with Philips Xpert MPD Pro X-ray diffraction, the selected area diffraction was investigated with a JEM-2010 transmission electron microscope, the depth contribution of elements was detected by PHI-610 auger electron spectroscopy, and the DSC-TG test was conducted with a STA409 simultaneous thermal analysis to study the thermo-stability of the nitride coating.

3. Oxidation behavior of the titanium alloy

Fig. 1 shows the SEM image of TC11 specimens under different oxidation conditions in air. After oxidation at 650°C for 100 h, loose and rough oxide scales are clearly observed, as shown in Fig. 1(a). With the temperature increasing, at 700°C for 100 h the oxidized surface is non-uniform, and some oxide particles penetrate the surface with obviously preferred growth, as shown in Fig. 1(b). In this case, Ti-rich oxides were measured. At 800°C, only for 10 h, the flaking oxide skin was observed as shown in Fig.1 (c) due to a severe oxidation reaction, and at this moment the oxide particles have rapid growth.

Surface energy spectrum analysis (Fig. 2 and Table 1) for the oxidized titanium alloy shows that the content of the aluminum is poor, with the Al/Ti ratio < 1. As the temperature increases, the content of aluminum becomes gradually higher, but in the selected area, the enrichment of titanium is clearly detected. At the top surface, it seems that in the alloys the titanium element has high diffusion velocity. There is low aluminum content (only 6.5 wt.%) in the titanium alloy during the oxidation process, and the substrate cannot be completely overcovered with the uniform Al_2O_3 film. Meanwhile, the Ti ion in TiO_2 has a higher self diffusion velocity, and interstitial Ti ions and oxygen vacancy are also common defects in titanium oxide, which would lead to the rapid growth of TiO_2 crystals [11].

The element distributions of oxidized alloys in the depth direction are presented in Fig. 3. It is clearly shown that the contents of oxygen, titanium and molybdenum hold the line with slight changes; the aluminum contents vary from outside to inside, and only concentrate at the top of the film. However, the density of titanium is always higher than that of aluminum in the depth direction. So based on the results of EDS and AES, it is concluded that the compound structures of Ti-rich and Al-poor oxides are formed during the high temperature process. In this case, the loose oxide layer with a mixture structure cannot prevent inner diffusion of oxygen; and oxide thickness would continue to increase.

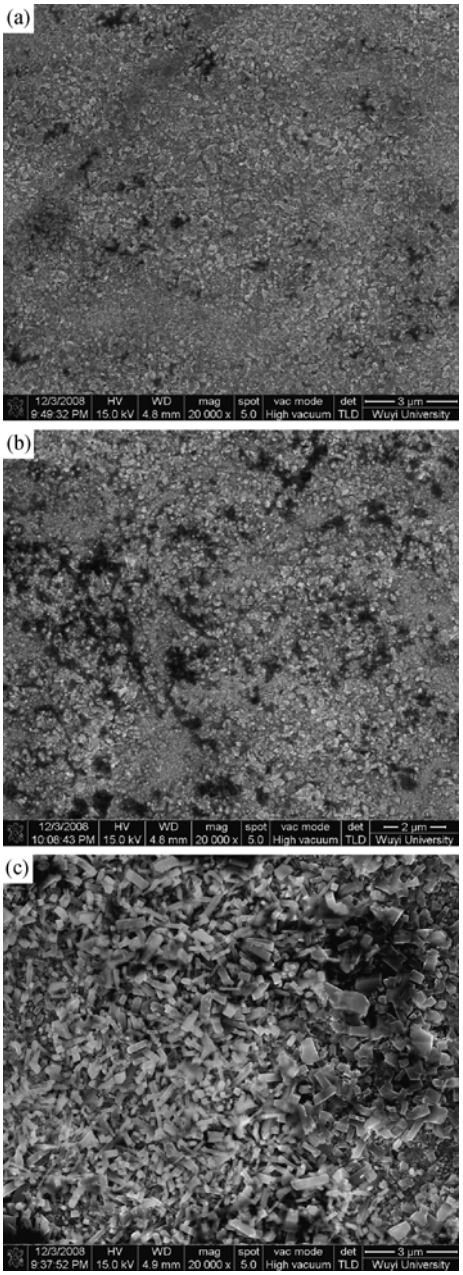

Fig. 1. High temperature surface oxidation morphologies of the oxidized titanium alloy: (a) 650°C / 100 h; (b) 700°C / 100 h; (c) 800°C / 10 h.

4. Performance analysis of protective coatings

4.1. Microstructure of $Ti_{0.5}Al_{0.5}N$ coatings

The typical AFM three-dimensional micrograph of a $Ti_{0.5}Al_{0.5}N$ coating deposited by the arc ion plating technique is shown in Fig. 4(a). The coating has a relatively smooth surface with some droplets, and no obvious cracks are observed, and the roughness of the $Ti_{0.5}Al_{0.5}N$ coating is 17.4 nm in an area of 1 μm × 1 μm. The cross-section view of the $Ti_{0.5}Al_{0.5}N$ coating is shown in Fig. 4(b). The compact grain

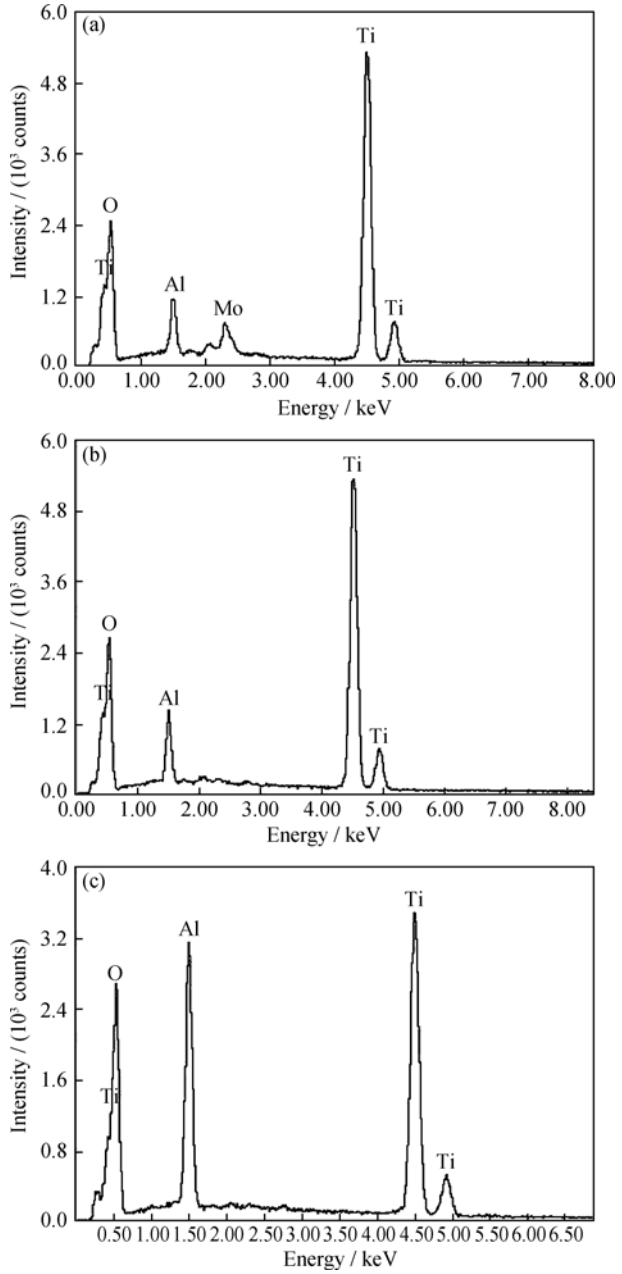

Fig. 2. EDS of oxidized TC11 alloy: (a) 650°C / 100 h; (b) 700°C / 100 h; (c) 800°C / 10 h.

Table 1. Element contents from EDS analysis results of TC11 alloy at different temperatures at.%

Heating condition	O	Al	Mo	Ti
650°C / 100 h	65.84	3.57	1.43	29.15
700°C / 100 h	66.92	4.56	—	28.52
800°C / 10 h	66.47	12.33	—	21.20

and homogeneous microstructure are obtained, there is good adhesion between the coating and substrate, and no peels are observed.

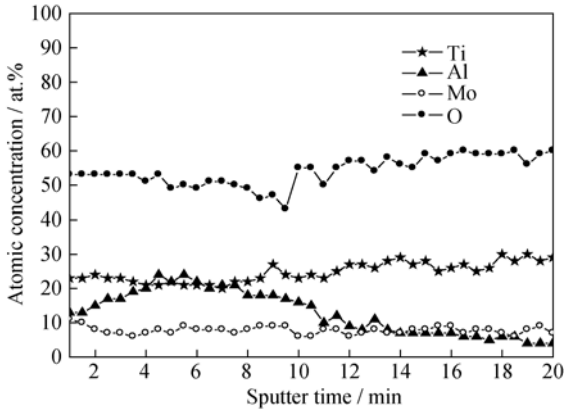

Fig. 3. AES profiles of oxidized TC11 alloy at 650°C.

The radius size of Al and Ti atoms are similar, at 0.143 nm and 0.146 nm respectively, so the position of the Ti atom in the Ti-N matrix can be replaced by an Al atom forming the TiN-based solid solution phase. The XRD results show that the coating phases are composed of the (Ti,Al)N phase as a B1-NaCl structure, and the preferred (111), (200), (220), and (222) diffraction peaks are noticed, while no AlN wurtzite structure is observed, as shown in Fig. 4(c). The sharp peaks indicate a well-crystallized structure. The lattice constant of $Ti_{0.5}Al_{0.5}N$ in this work is 0.419 nm, which is lower than that of pure TiN (0.424 nm). This phenomenon is commonly attributed to distort deformation due to different atom substitutions. While the decrease of lattice constant is also attributed to electron transport, when the replacement of Al occurs in the TiN matrix, the trend of charge transfer from the Ti 3d orbit to nitrogen atoms is weakened, thus the effective radius of nitrogen atoms decrease and then the crystal volume reduce [12]. To investigate the phase composition accurately, the selected area electron diffraction patterns are observed in Fig. 4(d), and the preferred (111), (200), (220), and (222) diffraction rings are also noticed. The (311) diffraction ring is not marked due to it being very close to the (222) ring, which is well in accordance with the XRD results. Coatings are characterized with a polycrystalline composition; from inside to outside, the ratio of the square ring radius agrees with 3:4:8:11:12, which indicates that the crystal structures are in keeping with a face-centered cubic lattice.

4.2. SEM and XRD of oxidized $Ti_{0.5}Al_{0.5}N$ coatings

Fig. 5 shows that at the range of 650°C to 800°C, the good oxidation stability is found, and the oxidized specimens coated with $Ti_{0.5}Al_{0.5}N$ in air exhibit smooth surface morphologies, very similar to the initial specimens, and the oxidizing cracks are scarcely observed. It is concluded that $Ti_{0.5}Al_{0.5}N$ coatings preserve their nitride performance without severe oxidation failure at this temperature. The phase composition of oxide layers formed during the oxida-

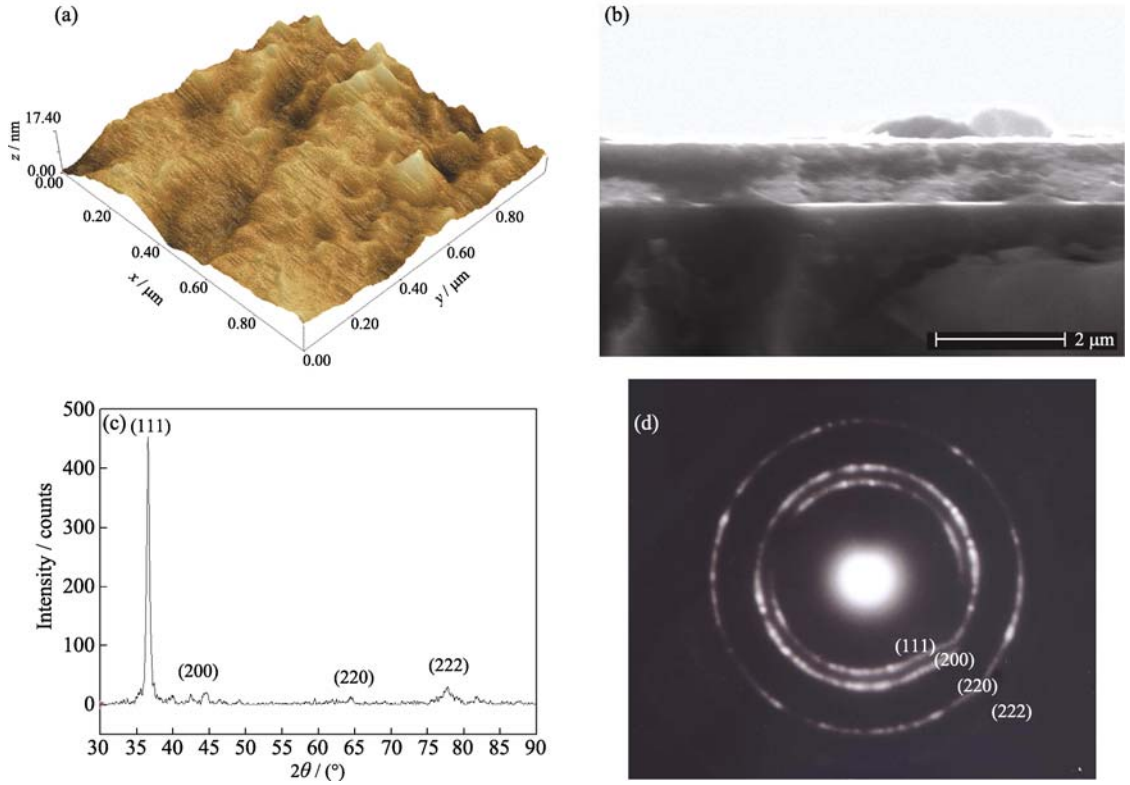

Fig. 4. Morphologies and microstructures of $Ti_{0.5}Al_{0.5}N$ coating: (a) AFM morphology; (b) Cross-section SEM morphology; (c) XRD pattern; (d) TEM diffraction rings.

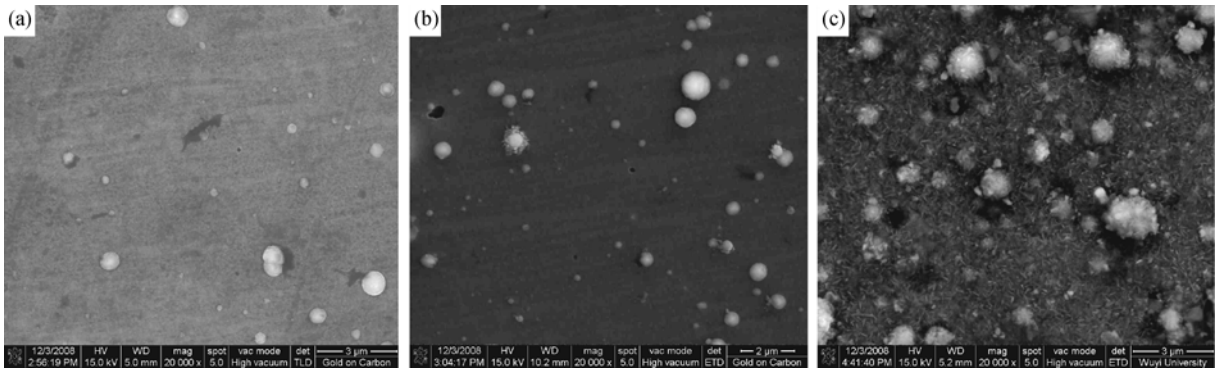

Fig. 5. Surface morphologies of oxidized $Ti_{0.5}Al_{0.5}N$ coatings: (a) 650°C / 100 h; (b) 700°C / 100 h; (c) 800°C / 30 h.

tion process is strongly dependent on oxidizing temperature.

Fig. 6 present the XRD patterns of as-deposited $Ti_{0.5}Al_{0.5}N$ coatings obtained in the different oxidation conditions in air. The coatings always keep the strong (111) preferred orientation even after oxidation at 650°C and 700°C for 100 h, and only a little of oxide phases are examined. The coatings show an improved oxidation resistance at a large temperature range, which may indicate that the Al ion can stabilize the valence electron of Ti ions in the Ti-Al-N system, which could reduce the reaction activity and then improve the oxidation resistance of nitride coatings [13]. Along with rising temperature, the diffraction intensity of the (111) peak slightly decreases, meaning that the stability of nitrides would be affected gradually with increasing oxidation rate. After oxidation at 800°C for 30 h, the coatings are partly oxidized, and the phases of Al and Ti oxides can be detected existing as α-Al_2O_3 and rutile TiO_2. Meanwhile, with the increasing oxidation temperature, the (111) diffraction peak in the $Ti_{0.5}Al_{0.5}N$ coatings have a slight shift due to phase transformation from TiAlN nitrides to oxides accompanied by the volume change and internal stress variation [14].

4.3. AES profile analysis

To explore the oxidation mechanism, especially in the

initial stage, whether the reaction rate is controlled by element diffusion in the layers was determined. The AES technique was used to detect the distribution of chemical elements [14]. The depth composition profiles of $Ti_{0.5}Al_{0.5}N$ coating oxidized at 800°C for 5 h are presented in Fig. 7, and it can be found that the selective oxidation of Al element occurs; there are an enrichment of Al, O and a depletion of Ti, N in the surface region.

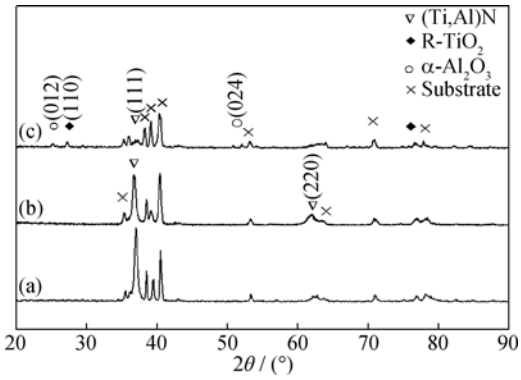

Fig. 6. XRD patterns of oxidized $Ti_{0.5}Al_{0.5}N$ coatings: (a) 650°C / 100 h; (b) 700°C / 100 h; (c) 800°C / 30 h.

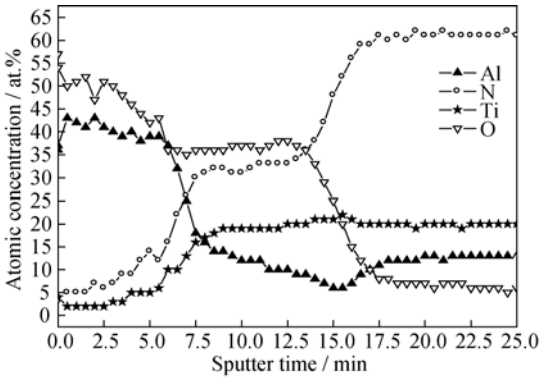

Fig. 7. Depth profiles of Ti, Al, N, and O elements in $Ti_{0.5}Al_{0.5}N$ coatings (800°C / 5 h).

The composition of the oxidized specimen is not uniform across the measured depth zone. Along the depth profile, the composition curves alter suddenly. Specifically, the ratio of aluminum and oxygen decreases, while the ratio variation trend of titanium and nitrogen is justly opposite. In brief, the concentration trend of Ti, Al, N, and O in the oxide layer is like a climbing or falling step shape. From outer to inner, the structure is as follows: Al-rich oxide scales, Ti-rich oxide scales mixed with a little Al oxides and residual nitride, nitride layer and substrate. A more interesting phenomenon found was that nitrogen has a tendency to escape from the coating during oxidation, which is close to experimental results published previously [15]. Once protective Al oxides are formed, the diffusion of oxygen and titanium ions would be obstructed, and the phase stability of the B1-NaCl structure for TiAlN is kept in a limited situation.

4.4. Oxidation kinetics

The oxidation at high temperatures is the thermal activation process, and the growing oxide film is affected by the migration of ions and electrons. Experimental results show that the weight gain for the TiAlN coating is in accordance with a parabolic law, indicating that the oxidation kinetics is controlled by the diffusion of reaction products in the oxide film. The dynamic relationship of weight gain and oxidation time is deduced by multiple regression models and verified by a related coefficient method. The kinetic curves are fitted to an equation $f(t) = kt^{0.5} + C$, where $f(t)$ is the weight gain per unit area, t is the oxidation time, and k is the parabolic rate constant shown in Fig. 8 and Table 2 specifically.

It is visibly noticed that the titanium alloys have a rather high mass gain, while low mass gain is observed for the $Ti_{0.5}Al_{0.5}N$-coated specimens during cyclic oxidation. From the XRD results, it is proven that the nitride coating can remain steady at 650°C and 700°C, and slight oxidation and diffusion occurs at this moment, so the values of the oxidation constant for $Ti_{0.5}Al_{0.5}N$ coatings are relatively small, at only about 0.0067 and 0.0078, respectively. With increasing temperature up to 800°C, as mentioned in AES in Fig. 7 above, the selective oxidation of Al elements occurs with preferred growth to form a compact Al_2O_3 film at the initial stage, which blocks the inward diffusion of oxygen and slows down the oxidation rate subsequently. At this time, oxide formation at the surface causes significant weight gain, the oxidation constant ascends to 0.0304, and the trend of weight gain is clearly lower than that of a single titanium alloy. Consequently, the coated specimens exhibit very low oxidation rates at the range of 650°C to 800°C. The protection is effective for the entire exposure period, which indicates that the $Ti_{0.5}Al_{0.5}N$ coatings improve the oxidation resistance of the titanium alloy.

4.5. Thermal analysis

Former oxidation studies mostly focused on the coating-substrate system, but under actual conditions, the oxidation resistance of coatings would also be affected according to the different substrate metals. These uncertain factors would make it difficult to research the intrinsic stability of nitride coatings used at high temperature. So special $Ti_{0.5}Al_{0.5}N$ coatings without substrates are obtained and heated from room temperature to 1200°C by a thermo gravimetric analysis system. Dry air is used to simulate the practical hot atmosphere environment and the heating rate is controlled to 20°C/min.

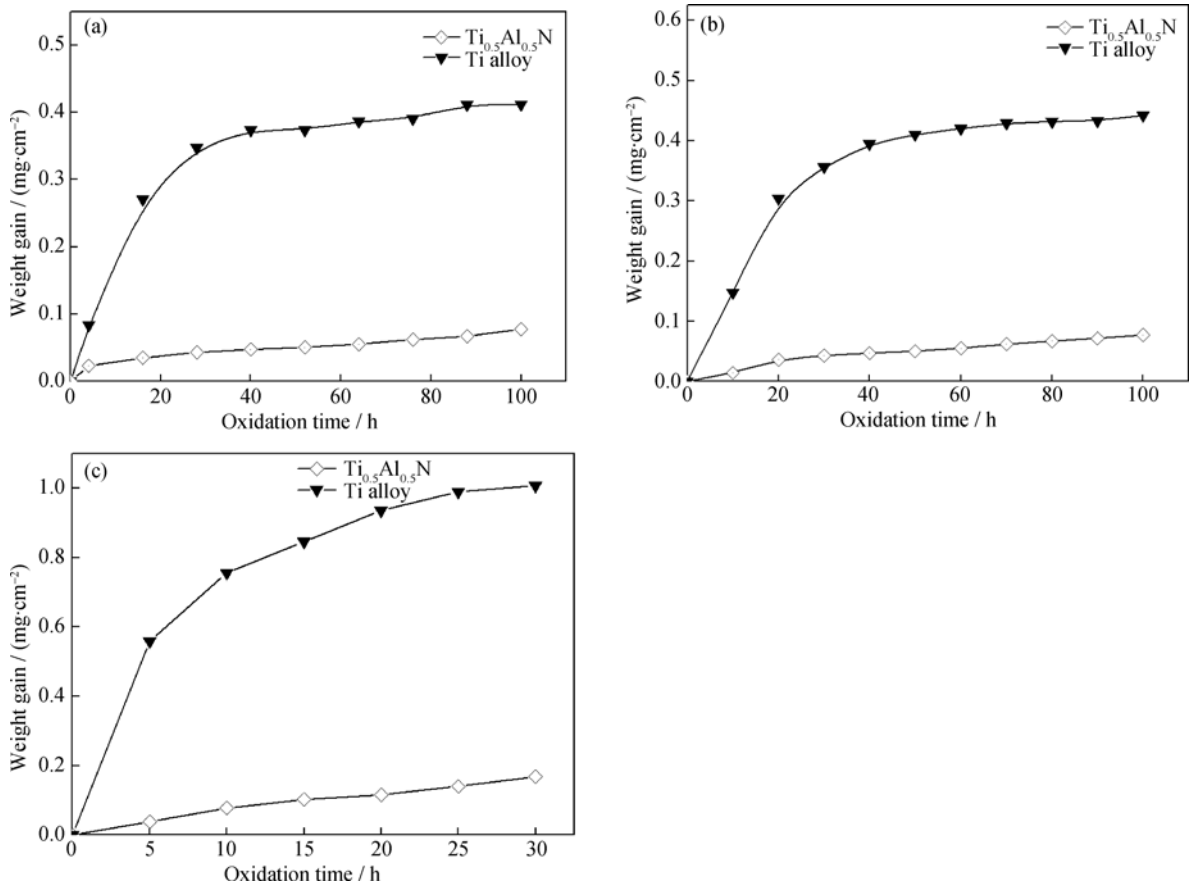

Fig. 8. Oxidation weight gains of $Ti_{0.5}Al_{0.5}N$ coatings at different temperatures: (a) 650°C / 100 h; (b) 700°C / 100 h; (c) 800°C / 30 h.

Table 2. Oxidation kinetic equations of $Ti_{0.5}Al_{0.5}N$ coatings

Specimens	Oxidation condition in air	Weight gain
$Ti_{0.5}Al_{0.5}N$-coated	650°C / 100 h	$f(t) = 0.0067\ t^{0.5} + 0.0046$
	700°C / 100 h	$f(t) = 0.0078\ t^{0.5} - 0.0028$
	800°C / 30 h	$f(t) = 0.0304\ t^{0.5} - 0.0134$

DTG (derivative thermo gravimetric analysis) curves exhibiting the chemical reaction rate are obtained. Thus, a comparison of the DSC (differential scanning calorimetry), TG (thermo gravimetric analysis) curves gives a possibility of determining phase transformation from chemical reactions, such as rutile and alpha Al_2O_3. In Figs. 9(a-b), the thermo analysis shows that low weight changes and weak heating effects are noticed from room temperature to 700°C, corresponding to the slight oxidation action. At this moment, the coatings are mostly characterized with the nitride structure, and this conclusion has been confirmed by SEM and XRD results. It is supposed that an aluminum element can increase the thermal stability of a Ti-N system. It is also estimated that the first stage of oxidation would be oxygen adsorption from $Ti_{1-x}Al_xN$ to $Ti_{1-x}Al_xNO_y$ only taking place on the topmost surface. As the temperature exceeds 800°C, the weight gain of the TG curve varies rapidly, this increase accounts for about 20%, and the maximum change of the DTG curve is at 887°C (Fig. 9(b)). Although the selective oxidation of Al element occurs at this stage, Al_2O_3 scales only partly protect the nitride in the dynamic heating condition. Outward diffusion of Al, inward diffusion of O and the escape of N synchronously take place. Accordingly, a strong exothermic peak is noticed, and the major exothermic spots are 877.0°C and 900.0°C, respectively, with –40.01 mW/mg and –42.12 mW/mg. While this thermal effect is closely related to the process of phase transformation, the nitrides are gradually destroyed by oxidation action, accompanied by mass Al_2O_3, TiO_2 and heat release.

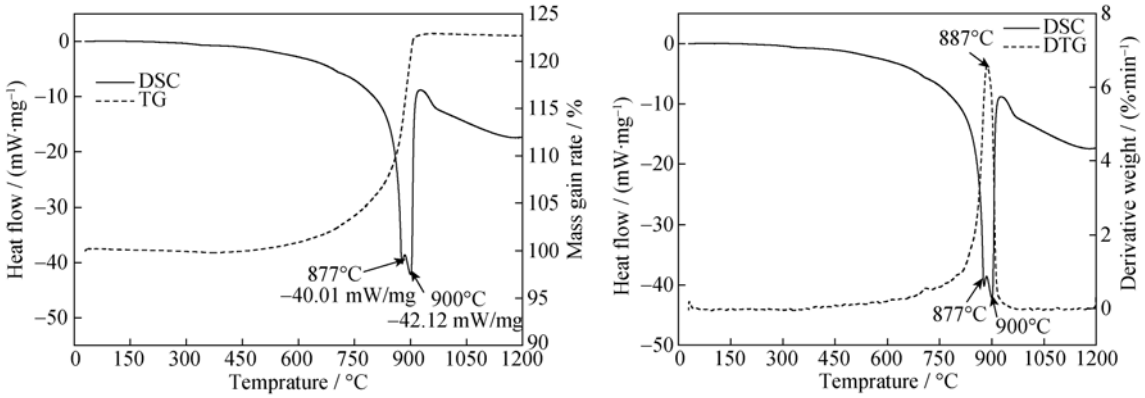

Fig. 9. Thermal curves of $Ti_{0.5}Al_{0.5}N$ coating: (a) DSC-TG; (b) DTG –DSC.

4.6. Coating oxidation mechanism

The oxidation mechanism is deduced based on the experiments using SEM, XRD, AES and TG-DSC. In the beginning, Al_2O_3 and TiO_2 scales have a trend of competitive growth. According to thermodynamics, aluminum has a preferential reaction with oxygen, however in real high temperature conditions, these competitive growths would be affected due to the different contents of Al and Ti at the initial reaction stage. If the aluminum content is lower in the coating or substrate, the specimens cannot be totally covered by a compact Al_2O_3 scale, and the following TiO_2 oxide would easily penetrate the Al_2O_3 layer with a mixture structure, which finally leads to protection failure, such as in titanium alloys. In the present paper, there is sufficient aluminum content to form dense aluminum oxides in a nitride coating. It can also be implied that an oxide/nitride interface is formed for a coated substrate due to selective diffusion espoused to oxygen conditions in high temperatures. The selective oxidation of Al element would generate a protective α-Al_2O_3 layer, which could reduce the activity of oxygen at the interface and change the distribution of oxides. Below the Al_2O_3 layer, Al contents are poor, while the mixed structure of the Ti-rich oxide zone is formed in the internal layer.

5. Conclusions

(1) $Ti_{0.5}Al_{0.5}N$ coatings prepared by arc ion plating exhibit a B1-NaCl structure, and Al replaces the position of the Ti atom in the Ti-N matrix to form the TiN-based solid solution phase.

(2) $Ti_{0.5}Al_{0.5}N$ coatings have a good resistance against oxidation. The selective oxidation of Al occurs, forming a stable α-Al_2O_3 layer upon exposure to high temperature conditions. The compact Al_2O_3 layers can block oxygen diffusion, thus protecting the subsequent nitride and substrate. Titanium alloys can be effectively protected by the Ti-Al-N system.

Acknowledgements

The SEM (NoVaTM SEM 430) and TG (STA409) measurements were performed in the Testing & Analysis Center of Wuyi University. The authors would like to thank Dr. LI Changming and Dr. LIU Zhiping for providing friendly support.

References

[1] Xu G.D. and Wang F.E., Development and application on high-temperature Ti-based alloys, *Chin. J. Rare Met.* (in Chinese), 2008, **32** (6): 774.

[2] Gurrappa I. and Gogia A.K., High performance coatings for titanium alloys to protect against oxidation, *Surf. Coat. Technol.*, 2001, **139**: 216.

[3] Zhao Y.G., Zhou W., and Qin Q.D., Effect of pre-oxidation on the properties of aluminide coating layers formed on Ti alloys, *J. Alloys Compd.*, 2005, **391**: 136.

[4] Gurappa I., Protection of titanium alloy components against high temperature, *Mater. Sci. Eng. A*., 2003, **356**: 372.

[5] Liu H.P., Hao S.S., Wang X.H., and Feng Z.X., Interaction of a near-α type titanium alloy with NiCrAlY protection coating at high temperatures, *Scripta Mater.*, 1998, **39**: 1443.

[6] Jindal P.C., Santhanam A.T., Schleinkofer U., and Shuster A.F., Performance of PVD TiN, TiCN, and TiAlN carbide tools in turning, *Int. J. Refract. Met. Hard Mater.*, 1999, **17**: 163.

[7] Harris S.G., Doyle E.D., and Vlasveld A.C., Influence of chromium content on the dry machining performance of cathodic arc evaporated TiAlN coatings, *Wear*, 2003, **254**: 185.

[8] Harris S.G., Doyle E.D., Vlasveld A.C., and Dolder P.J., Dry cutting performance of partially filtered arc deposited titanium aluminium nitride coatings with various metal nitride base coatings, *Surf. Coat. Technol*., 2001, **146**: 305.

[9] Weber F.R., Fontaine F., Scheib M., and Bock W., Cathodic

arc evaporation of (Ti,Al)N coatings and (Ti,Al)N/TiN multi-layer-coatings—correlation between lifetime of coated cutting tools, structural and mechanical film properties, *Surf. Coat. Technol*., 2004, **177**: 227.

[10] Ru Q., Hu S.J., Huang N.C., Zhao L.Z., Qiu X.L., and Hu X.Q., Properties of TiAlCrN coatings prepared by vacuum cathodic arc ion plating, *Rare Met.*, 2008, **27** (3): 251.

[11] Luridiana S. and Miotello A., Spectrophotometric study of oxide growth on arc evaporated TiN and ZrN coatings during hot air oxidation tests, *Thin Solid Film*, 1996, **290**: 289.

[12] Wahlstrom U., Hultman L., and Sundgren J.E., Crystal growth and microstructure of polycrystalline $Ti_{1-x}Al_xN$ alloy films deposited by ultra-high-vacuum dual-target magnetron sputtering, *Thin Solid Films*, 1993, **235**: 62.

[13] Zhou M., Makino Y., and Nose M., Phase transition and properties of TiA1N thin films prepared by r.f. plasma assisted magnetron sputtering, *Thin Solid Films*, 1999, **339**: 203.

[14] Ru Q., Hu S.J., Huang N.C., Zhao L.Z., Qiu X.L., and Hu X.Q., Resistance to high-temperature oxidation of arc ion plated TiAIN coating on heat-resisting titanium alloy, *Mater. Protect.* (in Chinese), 2007, **40**(1): 28.

[15] Vaz F. and Rebouta L., Thermal oxidation of $Ti_{1-x}Al_xN$ coatings in air, *J. Eur. Ceram. Soc*., 1997, **17**: 1971.